DOI: 10.3901/CJME.2009.05.***, available online at www.cjmenet.com; www.cjmenet.com.cn

Experimental and Numerical Investigation on a Centrifugal Pump under Air-Water Two-Phase Flow Condition

SI Qiaorui[1], BOIS Gerard[2]*, ZHANG Keyu[1], YUAN Shouqi[1]

1 *National Research Center of Pumps, Jiangsu University, Zhenjiang, China, 212013;*
2 *Lille Mechanics Laboratory, UMR CNRS 8107, Arts et Métiers ParisTech, Lille, France, 59046*

Received XXX; revised XXX; accepted XXX; published electronicallyXXX

Abstract: Experimental and numerical investigations have been performed on a single stage, single-suction, horizontal-orientated centrifugal pump under air-water two-phase non condensable flow conditions. Experimental test loop allows performing controlled values of air void fraction for different water flow rates and several rotational speeds. Global pump heads and efficiencies have been measured for several inlet air void fraction values at different rotating speeds up to pump performance breakdown. Similar laws under two-phase flow condition have been investigated at three selected rotating speeds. Numerical calculations have been also performed using URANS approach including *k-e* turbulence and inhomogeneous two-phase models for nominal rotational speed, the results of which are used to understand some specific experimental results that have been obtained. The results show that the pump performance degradation is more pronounced for low flow rates compared to high flow rates and the similarity laws can also be applied for air-water two phase flow conditions corresponding to the bubbly flow regime, when IVAF is small. Particle fluid model with interface transfer terms looks quite suitable to evaluate pump performance degradation up to IAVF values of 7%. Air bubbles distribute on suction side of the blade and are detained more and more inside the impeller channel near "wake" area when IAVF increase. Bubbles take over 60% part of the channel when IAVF increase to 7% in all three flow rates, which is the reason of the pump performance deterioration.

Key words: Two-phase flow, Centrifugal pump, Experiment, Computational fluid dynamics

1 Introduction

Centrifugal pumps are widely used in industrial applications, such as in waste water treatment, oil industry, food production, nuclear-power, heating installations, shipbuilding industry or chemical industry. In some case, air will enter into the liquid conveying pump. Centrifugal pumps are commonly designed for single phase flow only. It is already well known that pump both head and efficiency will decrease under two-phase mixture condition compared to single-phase one. The degree of the degradation depends on geometrical, physical and thermal conditions. Moreover, air-water flow may even cause damage to the pump. Thus, it is of great interest for engineers to understand and disclose the air-water flow in centrifugal pumps.

There is a continuing engineering and scientific request for advanced studies on pumps in two-phase operation. Experimental testing included measuring pressure heads, power consumption, flow rates, flow visualization, bubble size measurement in two phase flows, and void fraction distribution have been done by Murakami and Minemura[1, 2], Kim et al[3], Sato et al[4], Suryawijaya[5], Thum et al[6], Schäfer et al[7]. However, most of centrifugal pump impeller geometries that have been studied for two-phase regimes are designed with two dimensional blade sections. Modern computational fluid dynamics meanwhile offers some capacity to simulate the flow characteristic. However, reliable two-phase flow simulations are still quite difficult due to the complexity of the flow and again the lack of suitable validation data and benchmark experiments. A two-phase semi-empirical approach was first developed by Mikielewicz et al[8] for a given specific speed type of centrifugal pumps. Several one dimensional models based on homogenous gas-liquid mixture have also been proposed by Minemura et al[9, 10] Furuya et al[11], Clarke and Noghrehkar[12]. These models can be considered to be valid for low values of void fraction (max. 6%) and so, far from surge operating conditions. Numerical simulations using URANS approach have been also performed in order to determine local phenomena more precisely in such flow pattern. Caridad and Kenyery[13] simulated two phase flow in an electrical submersible pump (ESP) using a 3D CFD model. Barrios and Prado[14] studied the dynamic behavior of the multiphase flow inside an ESP by setting the bubble size through high speed camera measurement results. This

* Corresponding author. E-mail: Gerard.BOIS@ENSAM.EU
This project is supported by National Natural Science Foundation of China (Grant No. 51509108), Natural Science Foundation of Jiangsu Province (Grant No. BK20150516), China Postdoctoral Science Foundation Funded Project (Grant No. 2015M581735, 2016T90422) and Senior Talent Foundation of Jiangsu University (Grant No. 15JDG048).

numerical method get better fit to experiment results in ESP research field, which will help us apply it to centrifugal pumps investigation.

In the present paper, experimental and numerical comparisons results are presented on two- phase flow performance in a centrifugal pump designed with 3D impeller shape. Two different experimental procedures are presented which aim is to prevent too much result scattering due to flow instabilities that usually occur with two phase flow pump behavior. Numerical results have been performed using inhomogeneous model (instead of usually homogeneous model), for which each fluid possesses its own flow field and the fluids interact via interphase transfer terms and compared with overall experimental ones.

2 Pump Geometry and Test Rig Arrangement

A commercial single stage, single-suction, horizontal-orientated middle specific speed centrifugal motor pump from manufacturer Grundfos was used to process the measurement, whose casing is typically combined with a spiral-volute unvaned annulus. We suppose the best efficiency operating point as the design one. The design parameters of the pump are shown in Table 1.

Table 1 Pump Parameters

Parameters	Value
Flow rate Q_d/m^3 h^{-1}	40
Head H_d/m	22.5
Rotation speed n_d/ r·min^{-1}	2910
Blade number Z	6
Outlet Blade width b_2/mm	15.5
Suction pipe diameter D_s/mm	65
Outlet pipe diameter D_d/mm	50
Impeller inlet diameter D_1/mm	79
Impeller outlet diameter D_2/mm	140
Base diameter of volute D_3/mm	150

Test rig is shown on Figure 1. As shown in this open loop, air inject into the mixer by a compressor. Air flowrates are measured by micro-electro mechanical systems flow sensors, which could supply volume air flowrate value on standard condition (25℃, 101325Pa). Gas-liquid flow is sucked by pump from the mixer, go through the regulating valve and finally arrive the downstream tank. Air bubbles exhaust to the exterior space at this open tank and the left pure water run to the upstream tank. Water flowrate was measured by an electromagnetic flow meter set between upstream tank and the mixer. Air void fraction could be calculated. Pump head and efficiency also could be obtained followed the way in ISO 9906：2012. It has to be noticed that the inlet pipe loop in horizontal. Part of the inlet tubing is transparent. This allows to see a global rough view of bubbles size. At this step, only air volume flow rate is measured, bubble diameter distribution including bubble number per volume at pump inlet is not available. Measurements are performed using the followed procedures: a constant void fraction is set by changing the throttle vane position and consequently obtained the corresponding water flow rate. Measurement biggest uncertainties calculated by instrument precision are ± 1.6% error of pump head and 3% of air void fraction due to the effects of pump flow oscillations.

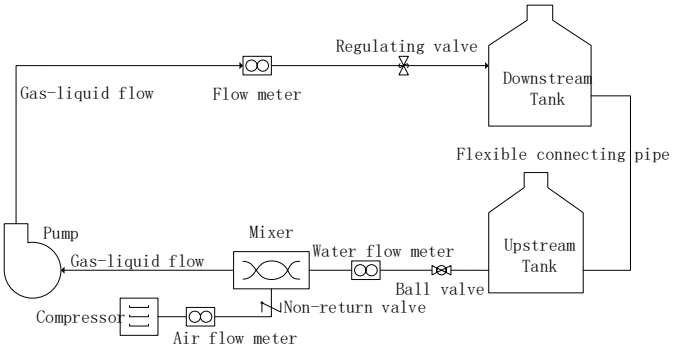

Fig. 1. Test rig

Pump performance measurement have been done for several impeller rotating speeds in order to plot all results using usual dimensionless coefficients for similar law investigation. For air-water two phase flow measurement, the test loop condition were that 2m water high level inside the tank, air inject the same direction with the water flow, 0.5mm diameter holes of four injecting tube around the mixer pipe. The water flow rate were kept constant, and the air injecting flow rate were changed to keep the air void fraction at 1%, 3%, 5%, 8%, 9%, 10% and more. Such pump performance measurement under two phase flow were done in three selected rotating speed.

3 Numerical Simulation Modeling

3.1 Calculation domains and meshes

The pump was divided into component parts such as the suction inlet, ring, pump impeller, volute and chamber to build a numerical model for a complete pump, as shown in Figure 2. This process would allow each mesh to be individually generated and tailored to the flow requirements in that particular component. The influence of boundary conditions was investigated to discard any effect on the numerical results, particularly on the inlet and outlet part. We extend these two parts to assume that the flow closed to inlet and outlet parts were in a fully developed condition.

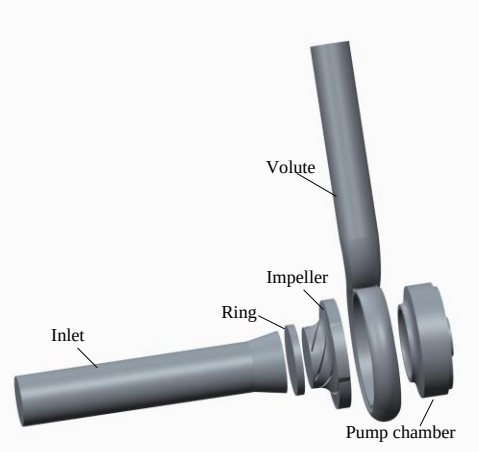

Fig. 2. 3D model of numerical domain

The grids for the computational domains were generated using the grid generation tool ICEM-CFD 14.5 with blocking method. The independence of the solutions from the number of grid elements was proven by simulating the flow field with different numbers of grid elements. Finally, the resulting pump model consisted of 2775915 elements was chosen for rotating and stationary domains in total. Structured hexahedral cells were used to define the inlet, impeller ring, impeller, chamber and volute domains, which had 422604, 42240，950976, 433656 and 926439 elements, respectively. The grid details in the rotating domain and the volute wall are partially shown in Figure 3.

Fig. 3. Details of grid view

3.2 Boundary condition and numerical models

Three-dimensional URANS equations were solved using the *k-e* turbulence mode, with boundary conditions of total pressure at the inlet and mass flow at the outlet. Smooth wall condition was used for the near-wall function. Inhomogeneous model also named the interfluid transfer model was chosen to adapt the Eulerian-Eulerian multiphase flow. In this model each fluid possesses its own flow field and the fluids interact via interphase transfer terms. Thus, this model provides one solution field for each of the separate phases. Transported quantities interact via interphase transfer terms. Furthermore, particle model is applied for the interphase transfer terms, which is suitable for modeling dispersed multiphase flow problems such as the dispersion of gas bubbles in a liquid. Bubble diameter set as 0.1mm or 0.2mm.

The interface between the impeller and the casing is set to "transient rotor-stator" to capture the transient rotor-stator interaction in the flow, because the relative position between the impeller and the casing was changed for each time step with this kind of interface. The chosen time step (Δt) for the transient simulation is 1.718×10^{-4}s for nominal rotating speed, which corresponds to a changed angle of 3°. Within each time step, 20 iterations were chosen and the iteration stops when the maximum residual is less than 10^{-4}. The convergence criterion for the transient problem is when the result have reached its stable periodicity. Ten impeller revolutions were conducted for each operational condition, and the last four revolutions results were kept for analysis.

4 Experimental Overall Pump Performance Results

Inlet and outlet total head is deduced from wall static pressure measurement and a one dimensional evaluation of kinetic pressure obtained from the volume flow rate measurements. Theoretical total head coefficient can be also obtained through global pump efficiencies, assuming no initial swirling flow at impeller inlet section. Pump performance results from numerical simulation is calculated by the average of one impeller revolution.

4.1 Single phase pump characteristics

Using head and flow coefficient from similarity laws, the following results on overall pump performances are shown in Figure 4, respectively for total head coefficient and theoretical total head coefficient. The following theoretical total head coefficient curves are built using classical head coefficient ψ_{th}. Five different rotational speeds have been chosen from nominal one (2910rpm) to the lowest one (1300rpm).

The Reynolds number value, defined in formula 1, based on the impeller outlet radius is relatively small for the last 3 pump rotational speed of 1800rpm, 1500 and 1300 rpm. If the relative outlet velocity should have been chosen, these values will below 1×10^6. This is probably the reason why the results on Figure 4(a) do not follow what expected according to similarity laws for these rotational speeds. However, the theoretical total head coefficients curve, Figure 4(b), exhibits a single curve for all rotational speeds. As a consequence, two phase flow measurements were carried out with three kinds of rotational speed that 2910rpm (nominal rotational speed), 2300 and 1800rpm (the critical rotating speed according to Reynolds number value).

$$R_e = \frac{2\pi n}{60}\cdot\frac{R_2^{\,2}}{\nu} \tag{1}$$

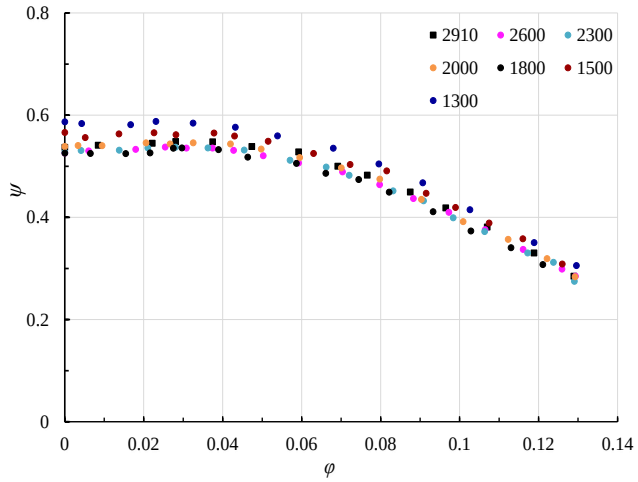

(a) Head

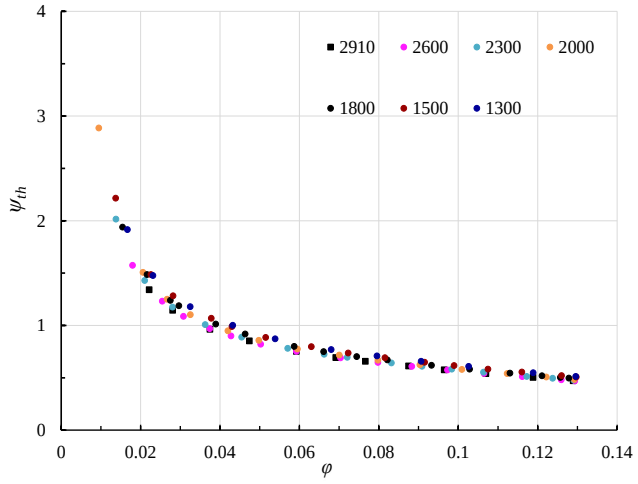

(b) Theoretical head

Fig.4. Pump head curve at different rotating speed under single phase condition

4.2 Two phase (air-water) pump characteristics

In the following, all results are presented for constant inlet air void fraction (IAVF) and water flow rate values, for three different rotational speeds excluding the two smaller ones for which Reynolds number values are below the critical one.

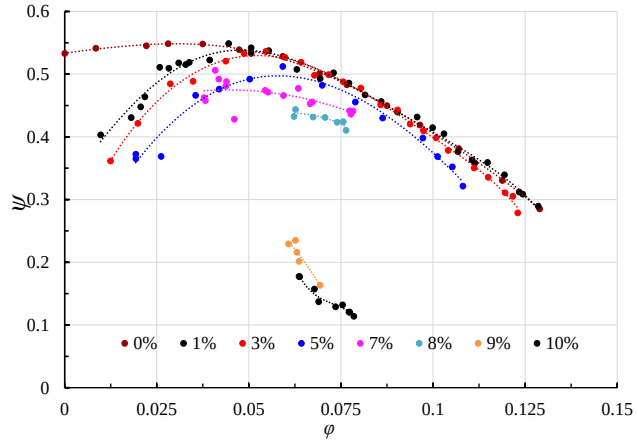

(a) Head

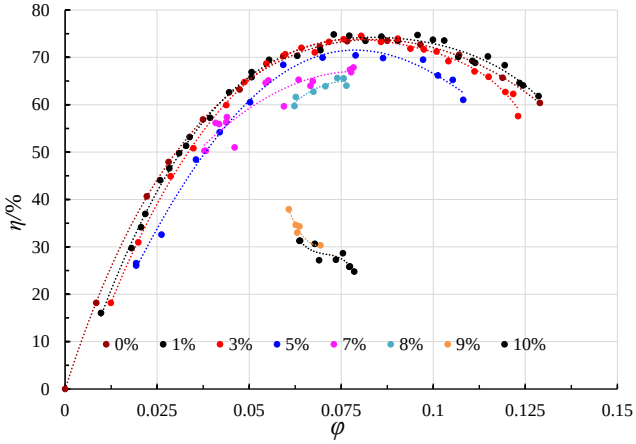

(b) Efficiency

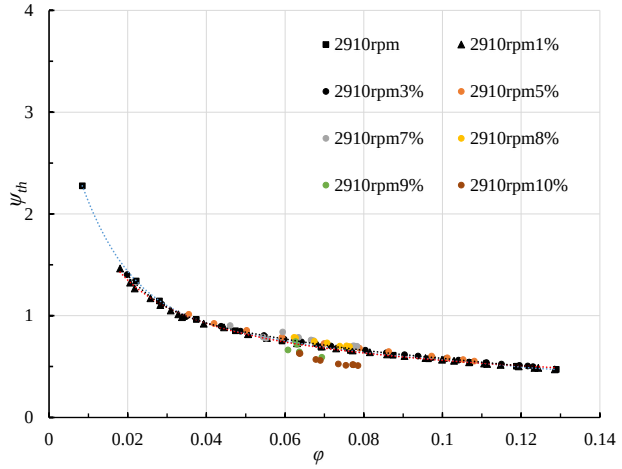

(c) Theoretical head at 2910rpm

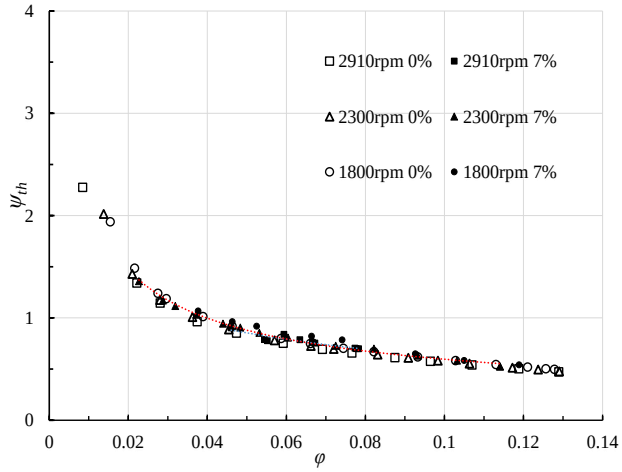

(d) Theoretical head under IAVF=0 and 7%

Fig.5. Pump performance curves under two phase flow conditions

Figure 5a and b show the pump performances under different IAVF for the nominal rotational speed of 2910 rpm. It can be seen that, as already pointed out by several previous researchers, that pump performances start to be significantly lower when void fraction is above 3% or 5%, depending on the water flow rate. A decrease of 20% of head compared with single phase shut-off conditions is achieved for all water flow rates below optimum conditions for void fraction going up to 7%. Lowest void fraction up

to 10% can be achieved without important pump surging for water flow rates coefficient around 0.06~0.077 (32~40 m^3/h). This value does not correspond to optimum pump efficiency point 0.087, which is reached for 45 m^3/h. On the efficiency curves, one can observed that maximum efficiency locations are displaced towards lower water flow rates when void fraction is increasing. This can be attributed to blockage effects at impeller inlet section which may affect the incidence angle values. Pump head and efficiency curves at the other two rotating speed give the same trend, but present the different values, which will discuss next.

Figure 5 (c) show a remarkable result, for which a unique curve is found using corrected two phase head and flow coefficients up to void fraction value of 8%. For the last two air void fraction, values of theoretical results are smaller than the IAVF below 8%. This may result from a change on the two phase relative flow angle at impeller outlet section, slip factors, or a bigger uncertainty on head measurement due to flow instabilities that start to be quite important for such void fraction values. Figure 5 (d) shows theoretical dimensionless head curves under IAVF=0 and 7% at rotating speed of 2910rpm, 2300rpm, 1800rpm. It exhibits a single curve for all rotational speeds. Moreover, curves at other IAVF that don't appear at this manuscript limited by the space also present the same law, which means that theoretical head is independent of fluid density duo to the two-phase flow. This result is an important one, since it validates all semi-empirical and one dimensional model assumptions that have been used for most of existing approaches that can be seen in the literature for such pump geometry with bubbly flow regime.

A second experimental set concerns the real head evolutions, obtained respectively for 0, 1%, 3%, 5% and 7% of air void fraction for three different rotational speeds. Total head coefficients versus flow coefficients are presented in Figure 6. Seen from the results, the similarity laws can also be applied for air-water two-phase flow conditions corresponding to the bubbly flow regime when IAVF are quite small (less than 3%). Pump heads exhibit increased difference when the IAVF increase. Moreover, results at 2300rpm and 1800rpm always show lower values than that at 2910rpm.

Pump performance degradation ratio ψ/ψ_0 has been obtained from previous results and plotted versus IAVF for three different flow coefficients, as shown in Figure 7. In each figure, the rotational speed is set as a parameter. It seems that rotational speed influences the head drop rate of the pump. The degradation ratio is biggest at 1800rpm under all three flowrate and become small when increase the rotating speed. The curves keep quite stable and close to 1 up to IGVF=5% at two bigger rotating speed under flow coefficients φ=0.077 and 0.058. When flow coefficient is decreasing, the head drop is more pronounced for decreasing rotational speeds.

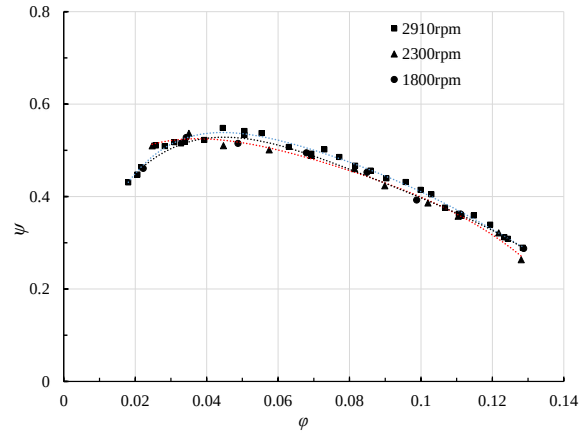

(a) IAVF=1%

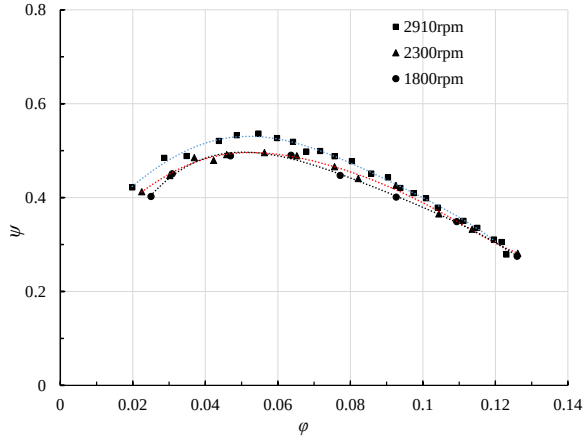

(b) IAVF=3%

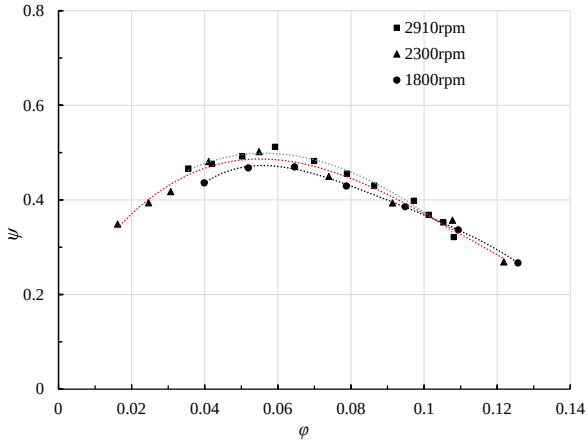

(c) IAVF=5%

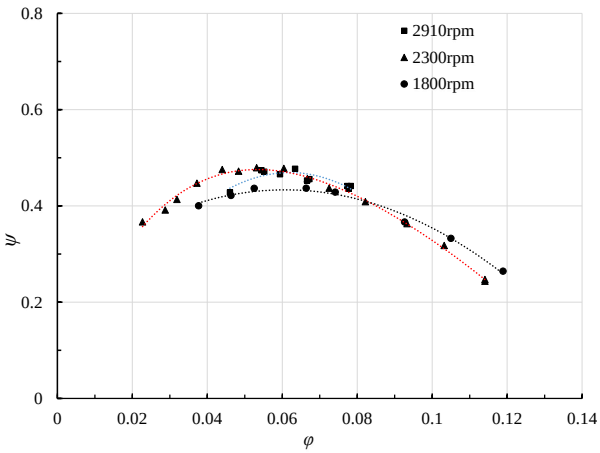

(d) IAVF=7%

Figure 6. Pump head coefficients comparison at different IAVF

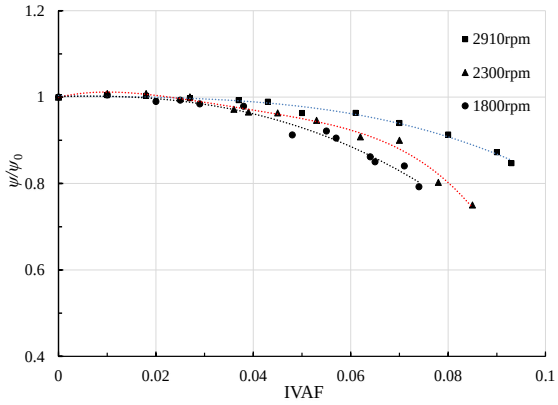

(a) Flow coefficient φ=0.077

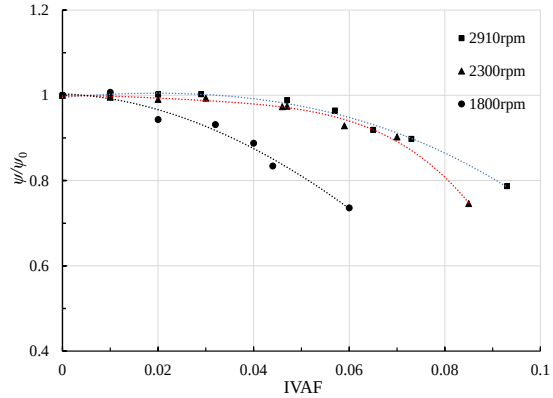

(b) Flow coefficient φ=0.058

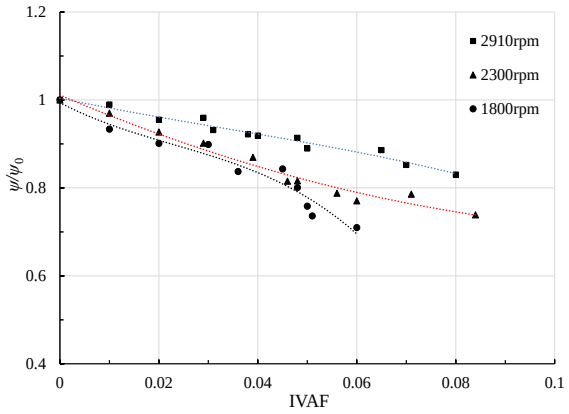

(c) Flow coefficient φ=0.040

Fig. 7. Pump performance degradation ratio

Compared to existing experiments such as presented in Minemura et al[9] paper, it can be pointed out that the head coefficient ratio remains at a quite high level for the present pump (even for IAVF=10%, with a small decrease of 5~6%) taking into account measurement accuracy. For higher values of IAVF (between 8 and 10%), the present experimental results do not follow the model proposed by Minemura et al and are close to the initial model made by Furuya et al[11]. In fact, the flow coefficient is an important parameter to deal with. So, it is believed that the flow incidence at impeller inlet must appear when building a model, because this may change the local void fraction which is an important parameter in order to predict the usual sudden head pump drop.

Below φ = 0.04, the ratio ψ/ψ_0 sharply decreases (more than 50%). This value of φ= 0.04 also corresponds roughly to a limiting value for which the theoretical head curve does not any more follow the theoretical straight line corresponding to the hypothesis of no inlet swirl. This sharp head drop, which is observed for low flow rate and high void fraction, is probably related to inlet swirl effects, combined with local reverse flows inside the impeller close to the inlet shroud area as already detected by Schäfer et al[7] in an another pump geometry.

5 Numerical Results

5.1 Pump performance comparison between the simulation and experiment

After the calculation finished, post solution of CFD were conducted in order to get overall pump performance information. All head and efficiency results were calculated by the average of the last four revolutions results. Comparison between the simulation and experiment when pump works at pure water condition are shown in Figure 8. For the CFD results, the delivery head was obtained from one averaged revolution of the unsteady calculation. Based on most conditions, the numerical head well agree with the corresponding experimental results. The agreement at the part-load operating points were better than that at the design and over-load operating points, which may be due to the neglected roughness. The maximum relative errors in the head and efficiency calculations were 3.8% and 0.3%, respectively. All of above means that the calculated domain, meshes, boundary condition and numerical turbulence models is suitable for the research.

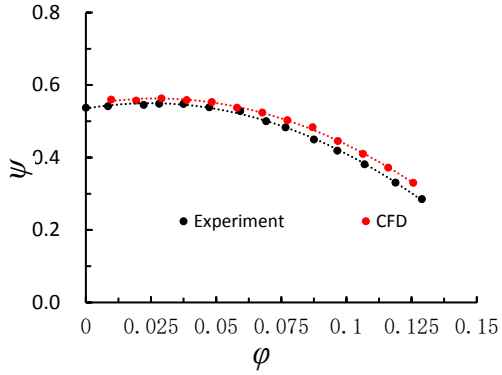

(a) Head

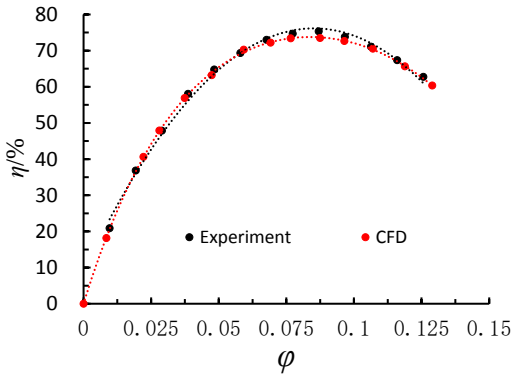

(b) Efficiency

Fig. 8. Performance curves of numerical simulation and experiment with IAVF=0

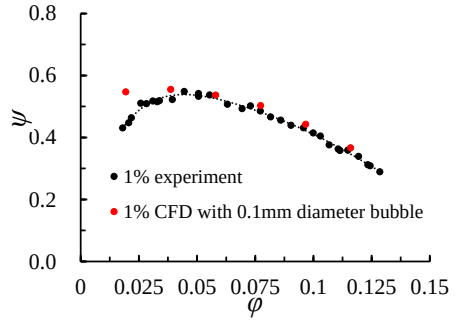

(a) IAVF=0.01

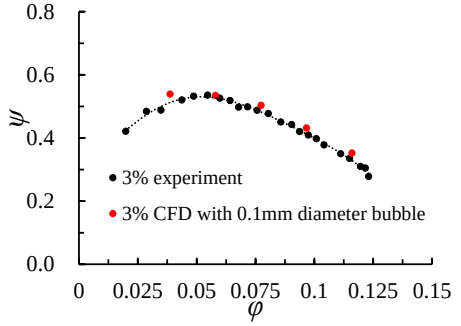

(b) IAVF=0.03

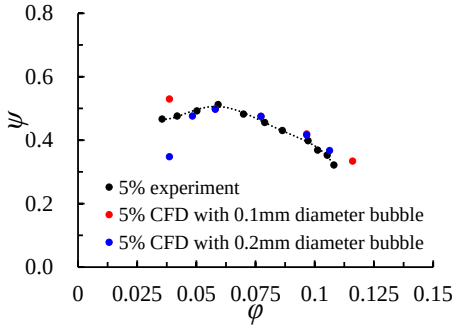

(c) IAVF=0.05

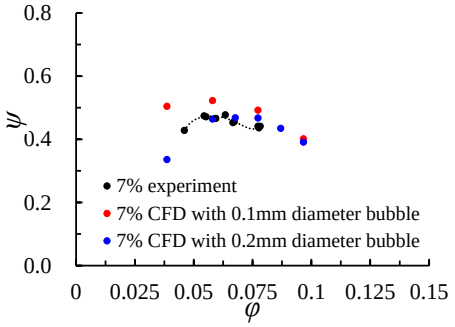

(d) IAVF=0.07

Fig. 9. Pump performance at different IAVF

Performance curves of numerical simulation and experiment with different AVF is shown in Figure 9. Numerical results show that the calculation is quite sensitive to initial bubble diameter value for small flow rates. Numerical results are quite comparable up to 7% of void fraction value for the adapted bubble diameter. From experimental investigation, it seems that pump performance is less sensitive to inlet bubble diameter values than numerical results. This result also needs more investigation in order to explain it. The simulation results are believable if choose the right initial bubble diameter.

5.2 Flow inside the impeller

Impeller is the most important energy conversion part of the pump. The transport gas-liquid ability of the pump is mostly depend on flow characteristic inside the impeller. Table 2 and Table 3 show air distribution on the blade surface and inside the impeller channel at three flow rates and three selected IAVF. It could be seen from it, air resides on the inlet leading edge near hub and outlet trailing edge near shroud when AVF is small. Air bubbles distribute on suction side of the blade and are detained more and more inside the impeller channel near “wake” area when IAVF increase. Air void fraction is bigger on pressure side than suction side in all three flowrates. Bubbles take over 60% part of the channel when IAVF increase to 7% in all three flowrates, which is the reason of the pump performance deterioration. Air bubbles have been also detected on blade pressure side from leading edge to the middle part. The outlet trailing edge, near shroud part of the impeller, presents the biggest α value.

6 Conclusions

Experimental overall pump performances have been performed under air water two phase conditions for a low specific centrifugal geometry, for a wide range of rotational speeds. Local flow pattern have been also obtained using CFD results in order to explain the head degradation level when IAVF was increased. The main results are the following:

(1) The similarity laws are valid for a range of rotational speed which is compatible with usual pump Reynolds number value above the critical one. The similarity laws can also be applied for air-water two phase flow conditions corresponding to the bubbly flow regime, when IVAF is small. For this flow regime, the theoretical head coefficient versus flow coefficient exhibits a single curve for all rotational speeds and IAVF values up to 7%.

(2) Pump performance degradation is more pronounced for low flow rates compared to high flow rates. The starting point of severe pump degradation rate is related a specific flow coefficient, which value corresponds to the change of the slope of the theoretical head curve.

(3) Compared with existing experimental results for 2D impeller shapes, the present 3D impeller pump geometry head degradation is quite small (less than 1%) within IAVF values below 5% around $0.75Q_n$ to Q_n.

(4) Local numerical results inside the impeller blade passages give some explanation about this last point and describe the air-water flow pattern change just before the experimental pump breakdown. Particle fluid model with interface transfer terms looks quite suitable to evaluate pump performance degradation up to IAVF values of 7%.

Table 2. Air distribution on blade under different IAVF

Flow rate	Scale	IAVF=1%	IAVF=5%	IAVF=7%
$0.75Q_n$		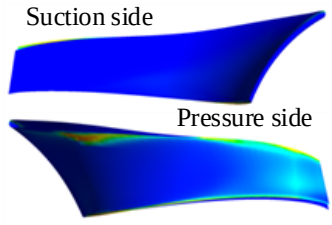	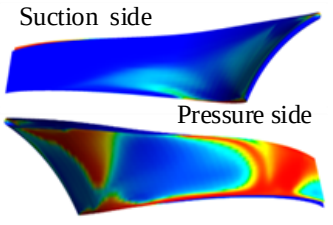	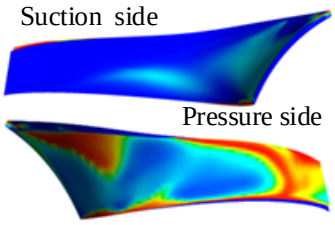
Q_n	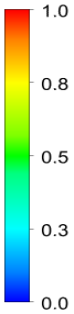	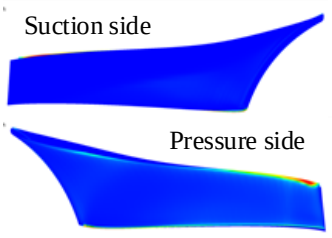	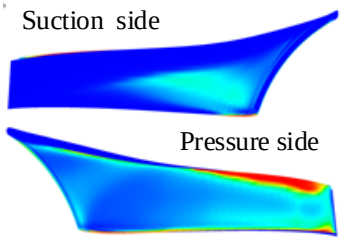	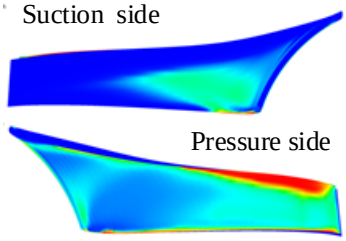
$1.25Q_n$		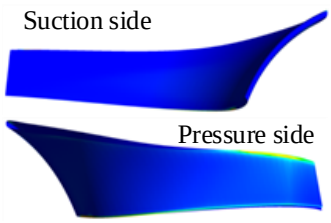	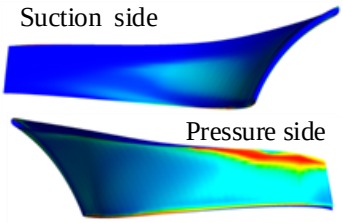	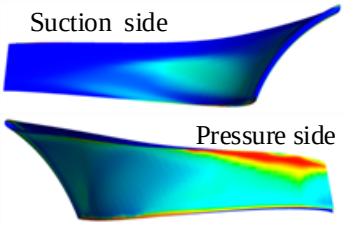

Table 3. Contour planes when α is above 20% for different IAVF values

Flow rate	Scale	IAVF=1%	IAVF=5%	IAVF=7%
$0.75Q_n$		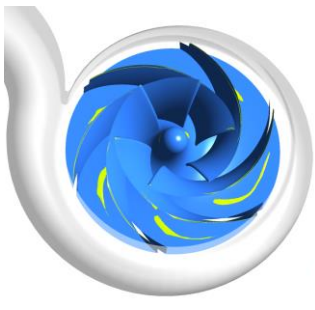		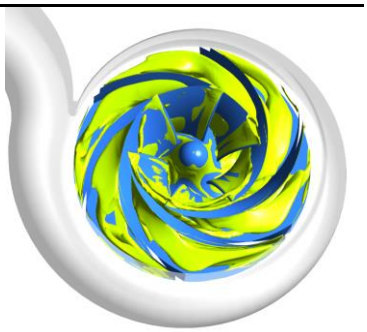
Q_n	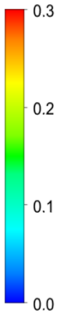		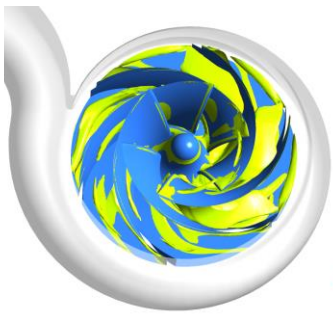	
$1.25Q_n$			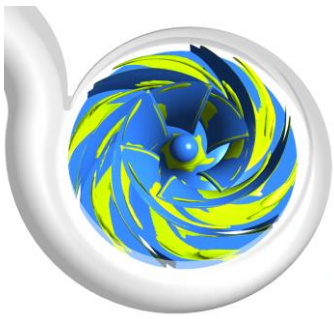	

References

[1] MURAKAMI M, MINEMURA K. Effects of entrained air on the performance of a centrifugal pump: 1st Report, Performance and flow conditions[J]. *Transactions of the Japan Society of Mechanical Engineers*, 1974, 17(110):1047-1055.

[2] MURAKAMI M, MINEMURA K. Effects of entrained air on the performance of centrifugal pumps: 2nd Report, Effects of number of blades[J]. *Bulletin of Jsme*, 1974, 40(330):459-470.

[3] KIM J H, DUFFEY R B, BELLONI P. On centrifugal pump head degradation in two-phase flow: Design method for two-phase flow in turbomachinery[C]//*ASME Mechanics Conference*. 26: 24-26.

[4] SATO S, FURUKAWA A, TAKAMATSU Y, et al. Air-water two-phase flow performance of centrifugal pump impellers with various blade angles[J]. *Bulletin of the Jsme*, 1996, 39(2):223-229.

[5] SURYAWIJAYA P, KOSYNA G, et al. Unsteady measurement of the static pressure on the impeller blade surfaces and optical observation on centrifugal pumps under varying liquid/gas two-phase flow conditions[J]. *Medicinski Arhiv*, 2003, 51(3-4):1-10.

[6] THUM D, HELLMANN D H, SAUER M. Influence of the patterns of liquid-gas flows on multiphase-pumping of radial centrifugal pumps[C]//*5th North American Conference on Multiphase Technology*. 2006: 79-90.

[7] SCHÄFER T, BIEBERLE A, NEUMANN M, et al. Application of gamma-ray computed tomography for the analysis of gas holdup distributions in centrifugal pumps[J]. *Flow Measurement and Instrumentation*, 2015, 46: 262-267.

[8] MIKIELEWICZ J, WILSON D G, CHAN T C, et al. A method for correlating the characteristics of centrifugal pumps in two-phase flow[J]. *Journal of fluids Engineering*, 1978, 100(4): 395-409.

[9] MINEMURA K, MURAKAMI M, KATAGIRI H. Characteristics of centrifugal pumps handling air-water mixtures and size of air bubbles in pump impellers[J]. *Bulletin of JSME*, 1985, 28(244): 2310-2318.

[10] MINEMURA K, KINOSHITA K, IHARA M, et al. Effects of outlet blade angle of centrifugal pump on the pump performance under air-water two-phase flow conditions[J]. *American Society of Mechanical Engineers*, New York, NY (United States), 1995.

[11] FURUYA O. An analytical model for prediction of two-phase (noncondensable) flow pump performance[J]. *Journal of Fluids Engineering*, 1985, 107:1(1):139-147.

[12] CLARKE A P, ISSA R I. Numerical Prediction of Bubble Flow in a Centrifugal Pump[J]. *Multiphase Flow*, 1995:175-181.

[13] CARIDAD J, KENYERY F. CFD Analysis of electric submersible pumps (esp) handling two-phase mixtures[J]. *Journal of Energy Resources Technology*, 2004, 126(2):99-104.

[14] BARRIOS L, PRADO M G. Modeling two phase flow inside an electrical submersible pump stage[J]. *Journal of Energy Resources Technology*, 2009, 133(4):227-231.

Biographical notes

SI Qiaorui (1986-), male, born in Henan province of China, is currently assistant professor of Jiangsu University. His research interests include unsteady flow, rotor-stator interaction in pump machinery.
Tel: +86-13655293881; E-mail: siqiaorui@ujs.edu.cn

BOIS Gerard (1950-), male, born in France, got full professor position in ENSAM at 2001 and is currently co-professor in Jiangsu University. His research interests include unsteady flow in turbine machinery.
Tel: +33-607437933; E-mail: Gerard.bois@ensam.eu

ZHANG Keyu (1992-), male, born in Hubei province of China, is currently a master student of Jiangsu University. His research topic is gas-liquid two-phase flow in centrifugal pump.
Tel: +86-18952840562; E-mail: zhangky189@163.com

YUAN Shouqi (1963-), male, born in ShangHai of China, is currently professor and president of Jiangsu University. His research interests include His research interests include the theory, optimization and design of fluid machinery.
Tel: +86 13705289318; E-mail: shouqiy@ujs.edu.cn

Appendix

a: Air void fraction $\alpha = \dfrac{Q_{air}}{Q_{air} + Q_{water}}$;

ρ: Density of mixed fluid $\rho = \rho_{water} \times (1-a) + \rho_{air} \times \alpha$;

v: Absolute flow velocity;

H: Pump head;

P: Shaft power;

η: Efficiency of the pump $\eta = \dfrac{\rho g Q_{water} H}{P}$;

φ: Flow coefficient $\varphi = Q/(2\pi \cdot R_2 \cdot b_2 \cdot u_2)$;

ψ: Head coefficient $\psi = gH/(u_2)^2$;

ψ_t: Theoretical head coefficient;

IAVF: Inlet air void fraction

R: Radius;

u: Circular velocity;

1: Impeller inlet;

2: Impeller outlet.